

# Synthesis of Dimethyl Hexane-1,6-dicarbamate with Methyl Carbamate as Carbonyl Source over MCM-41 Catalyst

Junya Cao,<sup>||</sup> Liyan Zhao,<sup>||</sup> Xiaoxuan Wang,<sup>||</sup> Shuang Xu, Yan Cao, Peng He, and Ligu Wang<sup>\*</sup>

Cite This: *ACS Omega* 2024, 9, 40485–40495

Read Online

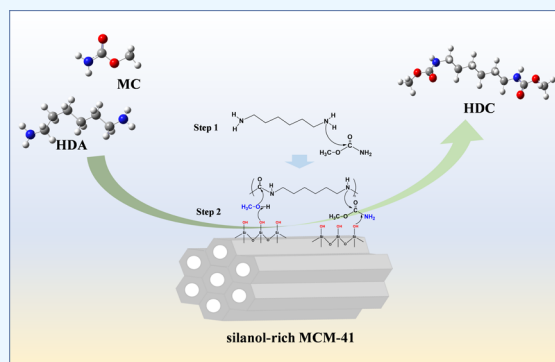
ACCESS |

Metrics & More

Article Recommendations

Supporting Information

**ABSTRACT:** Dimethyl hexane-1,6-dicarbamate (HDC), the vital intermediate for nonphosgene production of hexamethylene-diisocyanate (HDI), was effectively synthesized via carbonylation of 1,6-hexanediamine (HDA) using methyl carbamate (MC) as a carbonyl source over a silanol-rich MCM-41 catalyst. The effects of reaction conditions, including the reaction temperature, molar ratio of raw materials, methanol dosage, catalyst dosage, and reaction time, on the HDC yield were evaluated. Under the reaction conditions with a reaction temperature of 190 °C, a molar ratio of HDA, MC, and methanol of 1:6:50, a catalyst dosage of 10 wt %, and a reaction time of 3 h, the yield of HDC can reach as high as 92.6% with 100% HDA converted. Characterizations based on N<sub>2</sub> physical adsorption/desorption, scanning electron microscopy (SEM), X-ray diffractometry (XRD), NH<sub>3</sub>-temperature-programmed desorption (TPD), Fourier transform infrared spectroscopy (FTIR), and <sup>1</sup>H magic-angle spinning (MAS) NMR indicated that the abundance of silanol groups on the surface of MCM-41 probably resulted in the good performance of MCM-41. After five cycles of MCM-41, the HDC yield decreased from 92.6 to 67.9%, probably due to the loss of surface silanol groups and the carbon deposition on the catalyst as well as the particle agglomeration. The study on the substrate scope suggested that MCM-41 shows good-to-excellent catalytic performance in the synthesis of a variety of aliphatic and alicyclic dicarbamates.



## 1. INTRODUCTION

Dicarbamates are important fine chemicals and intermediates, which can be used not only in the synthesis of pesticides, medicines, and modified resins but also in the production of isocyanates via the nonphosgene method.<sup>1</sup> Nonphosgene synthesis of isocyanates has been widely investigated due to the advantage of avoiding the utilization of the extremely toxic phosgene.<sup>2,3</sup> Dimethyl hexane-1,6-dicarbamate (HDC), an attractive dicarbamate, is mainly used as the intermediate in the production of hexamethylene-diisocyanate (HDI) by the decomposition of carbamate.<sup>4–6</sup> HDI is an aliphatic isocyanate with excellent performance and can be extensively applied in high-end fields, such as automotive and aircraft coatings, refinish coatings, anticorrosion coatings, and biomimetic materials.<sup>7,8</sup>

Traditionally, oxidative carbonylation of amines,<sup>9,10</sup> reductive carbonylation of nitro-compounds,<sup>11,12</sup> and alcoholysis of urea<sup>13</sup> are the main methods of HDC synthesis. In the past years, increasing attention has been gained on the catalytic synthesis of HDC from 1,6-hexanediamine (HDA) and carbonyl sources, such as CO, urea, dimethyl carbonate (DMC), alkyl carbamate (AC), and even CO<sub>2</sub>.<sup>14,14</sup> Compared with other carbonyl sources, AC with low molecular weight, especially methyl carbamate (MC), has a higher reactivity. In addition, AC can be easily derived from the widely available urea or CO<sub>2</sub>.<sup>15,16</sup>

A variety of homogeneous catalysts, such as FeCl<sub>3</sub> and Y(NO<sub>3</sub>)<sub>3</sub>·6H<sub>2</sub>O, have been reported that can effectively catalyze the reaction of HDA and MC, giving HDC yields of 85–90%.<sup>17,18</sup> However, the homogeneous catalysts face the challenges of difficulty in separation and recovery. Several heterogeneous catalysts have been designed and applied to the carbonylation of HDA with AC. Han et al.<sup>19</sup> found that PbO<sub>2</sub> showed a good catalytic performance in the synthesis of HDC from HDA and MC. However, the catalyst was deactivated after use due to the transformation of PbO<sub>2</sub> into Pb<sub>2</sub>OCO<sub>3</sub>, which showed poor catalytic performance. Li et al.<sup>20</sup> investigated the performance of a series of heterogeneous catalysts (e.g., MgO, Fe<sub>2</sub>O<sub>3</sub>, Mo<sub>2</sub>O<sub>3</sub>, and CeO<sub>2</sub>) on the synthesis of HDC from HDA and MC. It was found that CeO<sub>2</sub> exhibits high catalytic activity. However, only an 83.1% HDC yield was obtained under the optimized conditions via a one-step reaction. Deng et al.<sup>21</sup> successfully prepared Ni/Fe<sub>3</sub>O<sub>4</sub> and found that the HDC yield reached as high as 96% after 5 h of

Received: April 9, 2024

Revised: August 16, 2024

Accepted: September 6, 2024

Published: September 16, 2024



reaction. Although a high HDC yield was obtained, the low reaction rate caused a long reaction time. The catalytic performance of the catalyst may be improved with an increased surface area. Wang et al.<sup>22,23</sup> found that Ti-based catalysts (hierarchical TS-1 and TiO<sub>2</sub>) may effectively catalyze the reaction of diamine and ethyl carbamate (EC). The good behaviors of these two Ti-based catalysts are suggested to be ascribed to their high surface area and abundant acid sites. Till now, the development of highly efficient catalysts is still the focus of research on the generation of HDC from HDA and MC. Several researchers highlighted the importance of nucleophilicity of amines during their carbonylation.<sup>21,22</sup> Therefore, catalysts with high surface area may promote the synthesis of HDC from HDA and MC.

MCM-41 has been applied as a catalyst in many reactions due to its high surface area, large pore volume, and well-defined pore structure.<sup>24</sup> In addition to these advantages, MCM-41 contains a large number of silanol groups,<sup>25</sup> which has been reported to exhibit strong adsorption to the -NH<sub>2</sub> groups in aromatic amines, thus promoting the activation of the amines.<sup>26</sup> In this study, the catalytic activity of MCM-41 on the carbonylation of HDA using MC as the carbonyl source was explored. The modified MCM-41 samples were prepared to investigate the effect of silanol groups on the performance of MCM-41. Combined with various characterization techniques, including N<sub>2</sub> physical adsorption/desorption, scanning electron microscopy (SEM), X-ray diffractometry (XRD), NH<sub>3</sub>-temperature-programmed desorption (TPD), and <sup>1</sup>H magic-angle spinning (MAS) NMR, the structure–performance relationship of MCM-41 samples was analyzed. The influence of the operational conditions for the carbonylation of HDA catalyzed by MCM-41 was studied. The catalysts used were characterized using various techniques, and the deactivation reasons were analyzed. Finally, the effect of MCM-41 on synthesis of a variety of aliphatic and alicyclic dicarbamates was investigated.

## 2. EXPERIMENTS

**2.1. Materials.** HDA (99.5%), MC (99%), toluene, trimethyl-chlorosilane (TMCS), and triphenyl-chlorosilane (TPCS) were all purchased from Shanghai Aladdin Biochemical Technology Co., Ltd. Anhydrous methanol (medicinal grade 99.5%), biphenyl (99.5%), and 4,4'-methylene-dianiline (MDA, gas chromatography >99.0%) were all purchased from Sinopsin Chemical Reagents Co. Ltd. Pentanediamine (PDA, 99.5%), *m*-benzoylamine (XDA, 99.0%), 1,3-cyclohexanedimethanamine (H<sub>6</sub>XDA, mixture of isomers, 95.0%), *p*-phenylenediamine (PPDA, 99.5%), 2,6-toluene diamine (2,6-TDA, 99.5%), 4,4'-methylenebis(cyclohexylamine) (H<sub>12</sub>MDA, mixture of isomers, 98.0%), and isophorone-diamine (IPDA, 99.0%) were all purchased from Shanghai Macklin Biochemical Co. Ltd. MCM-41, Al-MCM-41, HY, ZSM-5, and β-25 were purchased from Nanjing XFNANO Materials Tech Co. Ltd. SiO<sub>2</sub> and Al<sub>2</sub>O<sub>3</sub> were purchased from Shanghai Aladdin Biochemical Technology Co., Ltd. All chemicals in the experiments were of analytical grade and used without further purification unless otherwise specified.

**2.2. Preparation of Catalysts.** **2.2.1. Treatment of MCM-41 Calcined at Different Temperatures.** To differentiate the untreated MCM-41 from calcined MCM-41 and chlorosilane-modified MCM-41, MCM-41-U was used to denote the untreated MCM-41. The calcined MCM-41 sample was

obtained by heating 1.3 g of MCM-41-U to 200 or 300 °C in a muffle furnace with a heating rate of 5 °C/min and calcined at the desired temperature for 2 h. The calcined MCM-41 samples that were obtained at 200 or 300 °C were labeled as MCM-41-200 and MCM-41-300, respectively.

**2.2.2. Preparation of MCM-41 Modified by Chlorosilane.**<sup>27,28</sup> 1.3 g of MCM-41-U was pretreated in a vacuum dryer at 110 °C for 12 h. The pretreated MCM-41 sample was added into a suitable amount of the mixture of toluene and TMCS and then stirred at 80 °C for 12 h under a nitrogen atmosphere. The filter cake obtained after filtration was washed several times with acetone and ethanol. Finally, the TMCS-modified MCM-41 sample, which was labeled as MCM-41-M, was obtained by drying in a vacuum dryer at 110 °C for 12 h. Similarly, the TPCS-modified MCM-41, which was labeled MCM-41-P, was obtained by the same method by replacing TMCS with TPCS.

**2.3. Characterization of Catalysts.** The Brunauer–Emmett–Teller (BET) surface area, pore volume, and average pore diameters of the catalysts were obtained on a specific surface area and pore structure analyzer (Tristar II 3020, Micromeritics). The morphology of the catalyst was observed by a thermal field emission gun scanning electron microscope (SEM) (Gemini 300, Zeiss). The chemical composition and crystal structure of the catalysts were characterized by small-angle X-ray diffraction (SAXRD) on an X-ray diffractometer (Empyrean, Malvern PANalytical) using Kα irradiation over a 2θ range of 0.5–10°. The working voltage and applied current were 40 kV and 40 mA, respectively. The temperature-programmed desorption of NH<sub>3</sub> (NH<sub>3</sub>-TPD) of the catalyst was conducted on a temperature-programmed chemisorption analyzer (AutoChem II 2920, Micromeritics) with a thermal conductivity detector (TCD) to obtain the acidity properties of the catalyst, which was expressed by the number of NH<sub>3</sub> molecules per gram of catalyst. The structural information on various silanol groups of catalysts was determined by solid-state nuclear magnetic resonance hydrogen spectrum (<sup>1</sup>H MAS NMR), which was performed on an Agilent 600 MHz Premium COMPACT NMR Magnet.

**2.4. Synthesis of Dimethyl Hexane-1,6-dicarbamate.** All experiments were performed in a 100 mL stainless steel high-pressure reactor with magnetic stirring, which was heated by an electrical heating sleeve. The typical experimental procedures are listed as follows: 0.054 mol of methyl carbamate, 0.54 mol of methanol, 0.1 g of catalyst, and 0.009 mol of HDA were successively added into the reactor. The air in the reactor was replaced with high-purity nitrogen. The reactor was heated to 190 °C for 3 h with a rotating speed of 700 r/min. When the reaction was finished, the heating sleeve was turned off, and the reactor was cooled down to room temperature. Methanol was added to the reactor to dissolve the products, and then, the catalyst and the indissoluble solid residues were separated by centrifugation.

To understand the reaction pathway, the intermediate was collected and analyzed by FTIR. The main and byproducts were qualitatively analyzed by gas chromatography-mass spectrometry (GC-MS, Shimadzu).

The interaction between substrates and catalysts was investigated by *in situ* FTIR (Thermo Scientific Nicolet iS50) that was equipped with an MCT detector and an art photonics FPC-6 M Fiber Probe Coupler. The scanning was performed from 4000 to 400 cm<sup>-1</sup> with a resolution of 4 cm<sup>-1</sup>. The *in situ* FTIR spectra were collected under the conditions

of a reaction temperature of 190 °C, a molar ratio of HDA, MC, and methanol of 1:6:60, and a catalyst dosage of 10 wt % every 30 s for 1 h.

HDA and HDC were quantitatively analyzed by a gas chromatograph (GC-2014, Shimadzu) equipped with an RTX-5 (30 m × 0.25 mm × 0.25 μm) column and a flame ionization detector (FID) using N<sub>2</sub> as the carrier gas. The injection temperature and detector temperature were 240 and 250 °C, respectively. The temperature program for GC analysis was first held at 80 °C for 1.5 min and then heated to 200 °C at a rate of 20 °C/min and held for 10 min. The catalytic performance was evaluated by the conversion of HDA and yields of HDC, according to eqs 1 and 2. The detailed descriptions for the calculations are provided in the Supporting Information

$$\text{conversion (HDA) (\%)} = \frac{n_0(\text{HDA}) - n(\text{HDA})}{n_0(\text{HDA})} \times 100\% \quad (1)$$

$$\text{yield (HDC) (\%)} = \frac{n(\text{HDC})}{n_0(\text{HDC})} \times 100\% \quad (2)$$

where  $n_{0(\text{HDA})}$  is the molar amount of initial HDA,  $n(\text{HDA})$  represents the molar amount of unconverted HDA after reaction,  $n_{0(\text{HDC})}$  is the molar amount of the theoretically generated HDC that all HDA converted, and  $n(\text{HDC})$  represents the molar amount of generated HDC after the reaction.

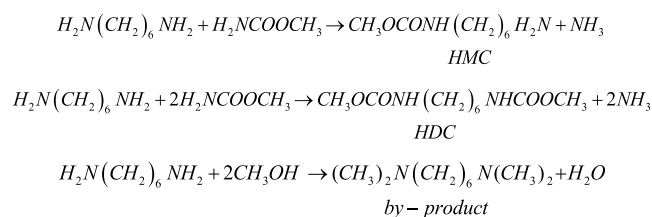
The leaching effect of the catalyst was investigated by a two-step experiment. The procedures were as follows: MCM-41-U was first soaked in methanol and heated at 190 °C for 1 h. Then, the MCM-41-U catalyst was removed, and HDA was added to the reactor to react for 0.5 h. A blank experiment was performed under the same operational conditions without a catalyst.

### 3. RESULTS AND DISCUSSION

**3.1. Reaction Pathway.** The carbonylation of aliphatic amine using alkyl carbamate as a carbonyl source via two steps with polyurea (PU) as an intermediate has been proposed.<sup>22</sup> A large amount of a white solid substance, which is insoluble in water and alcohol, was observed during the process. However, the solid was found to have disappeared at the end of the reaction. The white solid was collected, and its structure was detected by FTIR. The FTIR spectrum (Figure S1) indicates that the white solid that formed during the process was PU,<sup>29</sup> and the structure of PU is shown in Figure S2. The final reaction liquid was analyzed by gas chromatography-mass spectrometry (GC-MS), and the results are presented in Figure S3. The GC result shows that three peaks, located at the residence times of 8.68, 9.09, and 12.78 min, were observed. The MS results indicate that these three substances are methylated products, 1-(6-amino)-hexamethylene monocarbamate (HMC), and HDC, respectively. The reaction pathway was also investigated by *in situ* FTIR characterization. The trends of characteristic peaks of PU, HDA, and HDC over time under the condition without a catalyst are presented in Figure S4a. The results show that HDA was converted to PU at the beginning of the reaction, which was suggested by a weakening characteristic peak at 783 cm<sup>-1</sup> that belonged to the bending vibration of the N–H bond of HDA. The characteristic peak of PU, which is located at 1608 cm<sup>-1</sup> and belongs to the telescoping vibrations of the C=O bonds, became increasingly

obvious within 25 min of the reaction and then slightly decreased. Therefore, it is believed that the carbonylation of HDA using MC as a carbonyl source catalyzed over MCM-41 proceeds by first generating PU intermediates through the reaction of HDA with MC and then further undergoing alcoholysis to generate HDC. Similar results have been observed in the reported results.<sup>22</sup> The possible main and side reactions are listed in Scheme 1

#### Scheme 1. Possible Main and Side Reactions of HDA Carbonylation Using MC as a Carbonyl Source



**3.2. Catalyst Screening.** The catalytic performance of HY, Al-MCM-41, ZSM-5, β25 (four silica-aluminum molecular sieves), MCM-41-U (one silica molecular sieve), SiO<sub>2</sub>, and Al<sub>2</sub>O<sub>3</sub> was evaluated in this work, and the results are presented in Figure 1.

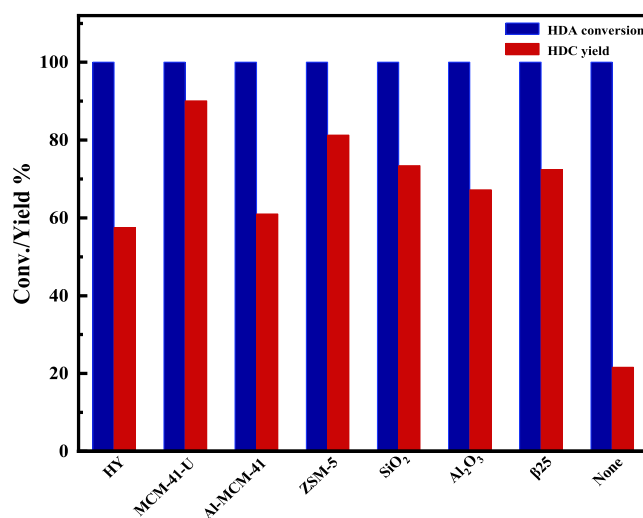


**Figure 1.** Effects of different catalysts on the carbonylation of HDA. Conditions:  $n_{\text{methanol}}/n_{\text{MC}}/n_{\text{HDA}} = 60:6:1$ , catalyst dosage = 10 wt % of HDA, temperature = 190 °C, time = 3 h.

As can be seen in Figure 1, HDA conversions for the reaction with and without a catalyst were both 100%, indicating that HDA was easy to be converted. Although HDA can be completely converted even under noncatalytic conditions, the yield of HDC was only 21.6% due to the severe side reactions. When the catalyst was utilized, the yield of HDC was significantly improved, ranging from 57.5 to 90.1%. Among the screened catalysts, MCM-41-U, a pure silica mesoporous molecular sieve, showed the best performance. MCM-41-U has a large surface area and pore size, which may provide more active sites,<sup>30</sup> leading to a high HDC yield. In addition, it is hypothesized that the highest catalytic activity of MCM-41-U may also be related to its abundant silanol groups on the surface, which has been reported and studied extensively.<sup>31,32</sup> To further confirm the roles of the silanol

groups of MCM-41-U on the catalytic performance, MCM-41-U was modified by calcination and chlorosilane pretreatment to reduce its silanol groups. Four modified MCM-41 catalysts, namely, MCM-41-200, MCM-41-300, MCM-41-M, and MCM-41-P, were prepared and characterized.

**3.3. Effect of Silanol Groups on the Catalytic Performance of MCM-41.** 3.3.1. *Characterization of MCM-41 Samples.* The five MCM-41 samples were characterized by XRD, as shown in Figure 2.

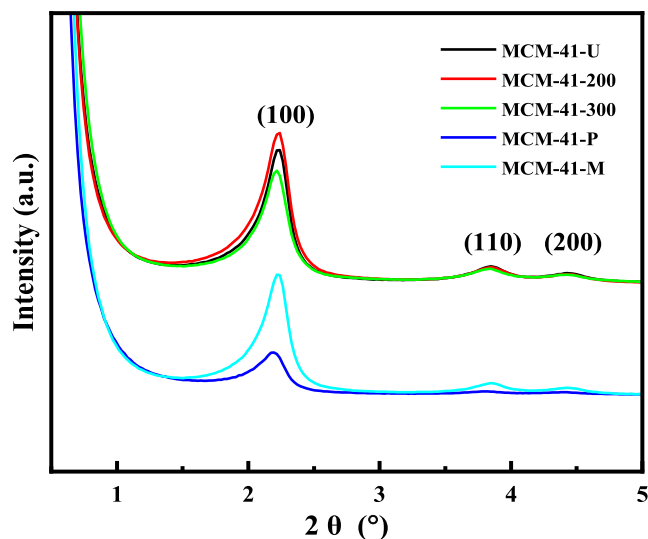


Figure 2. XRD patterns of five MCM-41 samples.

The peaks at  $2\theta$  of 2.24, 3.85, and 4.45° were attributed to the (100), (110), and (200) planes of MCM-41, respectively, indicating that MCM-41 has an ordered mesoporous structure with hexagonal cells.<sup>33</sup> The intensity of diffraction peaks at (100), (110), and (200) planes of MCM-41-200, MCM-41-300, and MCM-41-M was similar to those of MCM-41-U, suggesting that the highly ordered structure of MCM-41 was maintained after calcination and TMCS modification. The diffraction peaks of MCM-41-P at the (100), (110), and (200) planes were significantly weakened, which may be attributed to a poorly ordered structure and a destroyed pore structure after TPCS modification.

The  $N_2$  adsorption/desorption isotherms of MCM-41-U and modified MCM-41 catalysts are presented in Figure 3. The information about specific surface areas, pore volumes, and average pore sizes of the catalysts is listed in Table 1. As indicated by Figure 3, the nitrogen adsorption/desorption isotherms of several samples all belonged to type IV with a narrow pore size distribution (shown in Figure S5), which was consistent with the characteristics of MCM-41.<sup>34,35</sup> It is found that the pore properties of MCM-41 did not change significantly after calcination at 200 or 300 °C. The calcination at high temperatures resulted in slightly increased specific surface areas of MCM-41-200 and MCM-41-300. The modification of chlorosilane showed a pronounced effect on the pore structure of MCM-41. The pore volumes and pore sizes of MCM-41-M and MCM-41-P decreased significantly after chlorosilane modification, which may be ascribed to the successful penetration of TMCS and TPCS into the pores to form a Si–O–Si(CH<sub>3</sub>)<sub>3</sub> or Si–O–Si(Ph)<sub>3</sub>, respectively.<sup>32,36</sup>

The morphologies of the five MCM-41 samples were observed by SEM, and the SEM images are shown in Figure 4.

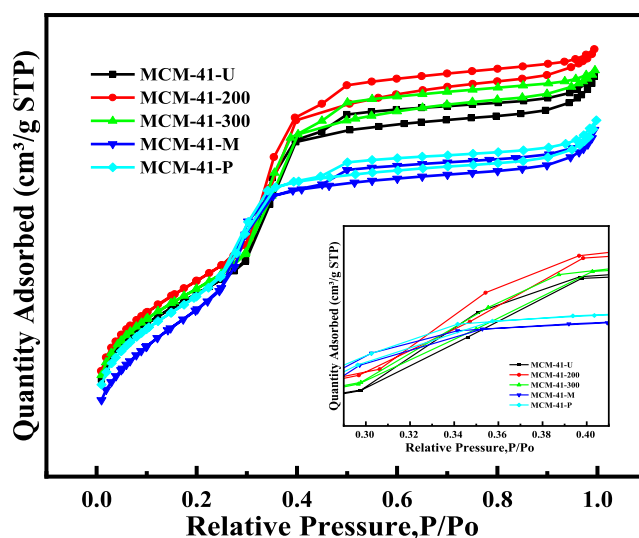


Figure 3.  $N_2$  physical adsorption/desorption isotherms of five MCM-41 samples.

Table 1. Textural Properties of MCM-41 Samples

entry	catalysts	$S_{BET}$ (m <sup>2</sup> /g)	pore volume (m <sup>3</sup> /g)	pore size (nm)
1	MCM-41-U	1021.55	0.87	2.90
2	MCM-41-200	1091.52	0.93	2.89
3	MCM-41-300	1052.30	0.88	2.87
4	MCM-41-M	1044.97	0.76	2.65
5	MCM-41-P	1048.01	0.77	2.95

As can be seen in Figure 4a, the particles of MCM-41-U were irregular and dispersed, which was consistent with the reported results.<sup>37</sup> Figure 4b,c shows that the high-temperature calcination has an insignificant influence on the morphology of MCM-41, but the particle sizes of MCM-41-200 and MCM-41-300 were slightly larger than that of MCM-41-U. The particle sizes of MCM-41 also were increased after chlorosilane modification, as presented in Figure 4d,e. In addition, slight particle agglomeration was observed for MCM-41-P.

It has been reported that catalysts with a high number of acid sites favor the formation of N-substituted carbamates using alkyl carbamates as the carbonyl source.<sup>22</sup> The number of acid sites of the five MCM-41 catalysts was determined by  $NH_3$ -TPD. As shown in Figure 5, an intense peak at a low-temperature range from 50 to 150 °C was observed for all samples in the spectra, indicating the presence of weak acid sites, which may be oriented from the silanol groups on the surface of the catalyst.<sup>38</sup> MCM-41-U had the highest acid site concentration (3.74 mmol of  $NH_3$ /g of catalyst), followed by MCM-41-200 (2.78 mmol of  $NH_3$ /g of catalyst) and MCM-41-300 (2.19 mmol of  $NH_3$ /g of catalyst). The decrease in acid site concentration after high-temperature calcination may be related to the removal of silanol groups on the surface of MCM-41.<sup>39</sup> After chlorosilane modification, the acid site concentration of MCM-41 decreased significantly, particularly with regard to MCM-41-P, whose concentration was only 0.19 mmol of  $NH_3$ /g of catalyst. The acid site concentration of MCM-41-M was 1.05 mmol of  $NH_3$ /g of catalyst. The extremely low acid site concentration may be attributed to the fact that the chlorosilane successfully entered the pore of MCM-41 and then interacted with Si–OH, thereby changing its surface acid properties.

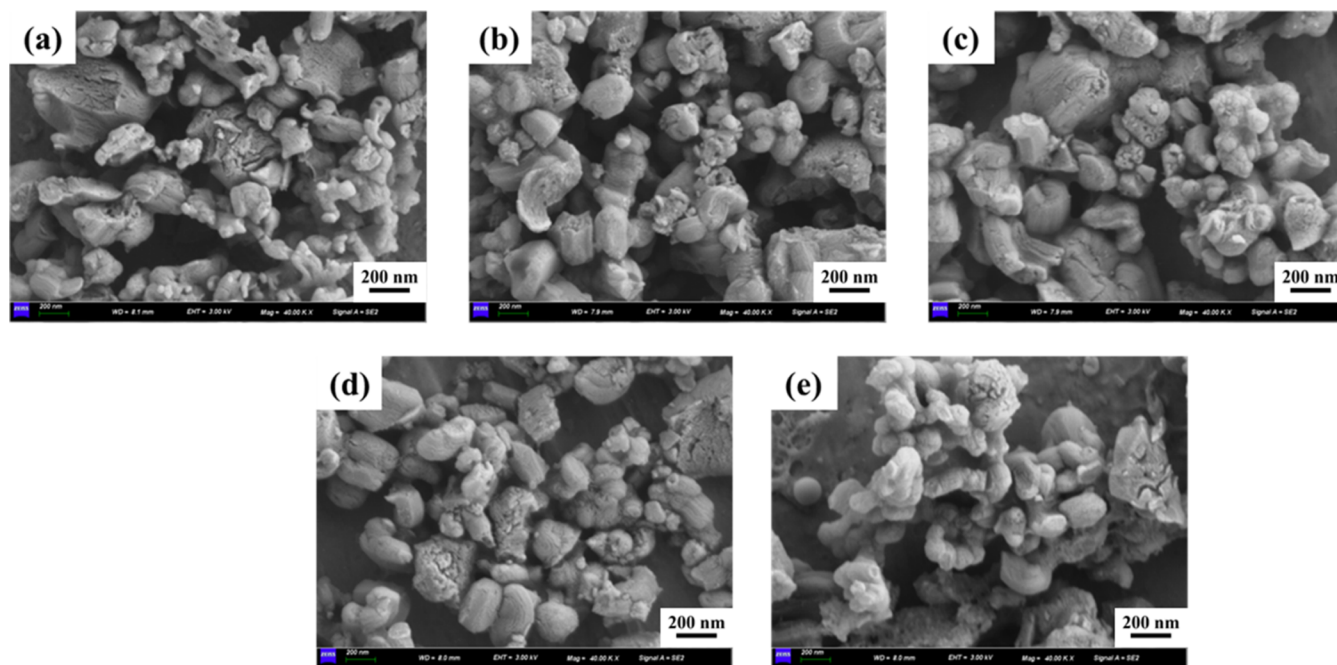


Figure 4. SEM image of (a) MCM-41-U, (b) MCM-41-200, (c) MCM-41-300, (d) MCM-41-M, and (e) MCM-41-P.

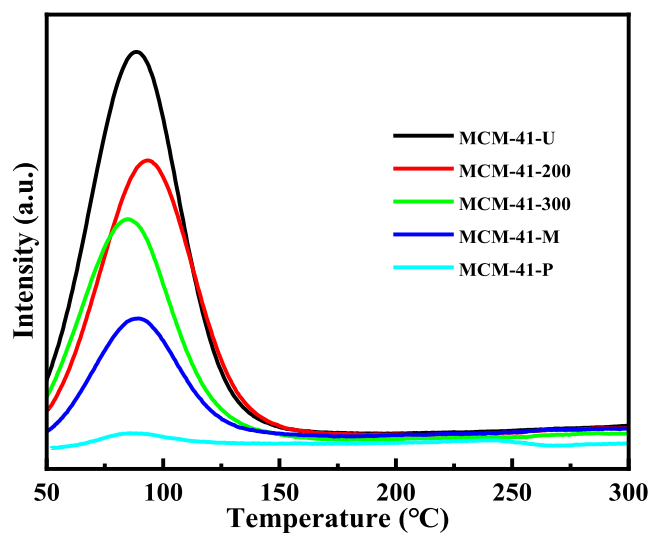


Figure 5.  $\text{NH}_3$ -TPD spectra of five MCM-41 samples.

$^1\text{H}$  MAS NMR spectra can provide structural information of various silanol groups and be widely used to investigate the changes of silanol groups on the surface of solid acids.<sup>40,41</sup> Five MCM-41 catalysts were characterized by  $^1\text{H}$  MAS NMR, and the results are shown in Figure 6. The MCM-41-U had a broad peak at  $^1\text{H}$  chemical shift of 4.44 ppm, which may be attributed to the silanol group-forming hydrogen bonds with water.<sup>40,42,43</sup> After the catalyst was calcined at 200 °C, the area of the main peak decreased and the peak location moved to 2.79 ppm. It is suggested that this peak belongs to the poly hydrogen-bonded vicinal Si-OH groups.<sup>40</sup> When the calcination temperature was increased to 300 °C, the main  $^1\text{H}$  chemical shift peak of MCM-41-300 further moved to 1.87 ppm, which may be ascribed to the isolated silanol group.<sup>43</sup> The shift of the  $^1\text{H}$  chemical shift peak after calcination may be attributed to dihydroxylation.<sup>44</sup> It has been reported that hydrogen-bonded silanol groups can be substantially removed and/or trans-

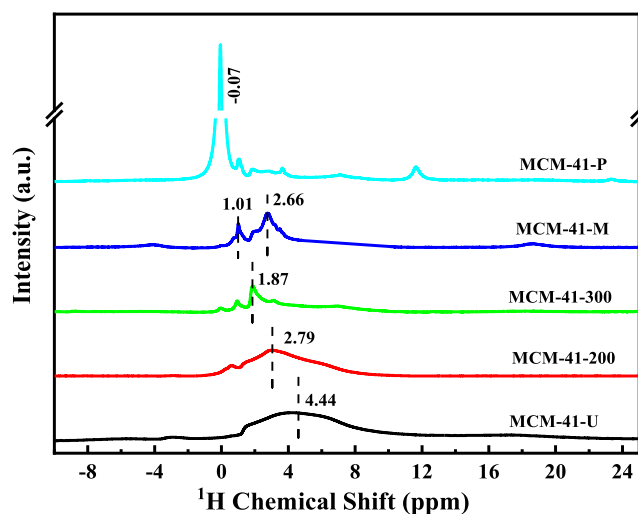
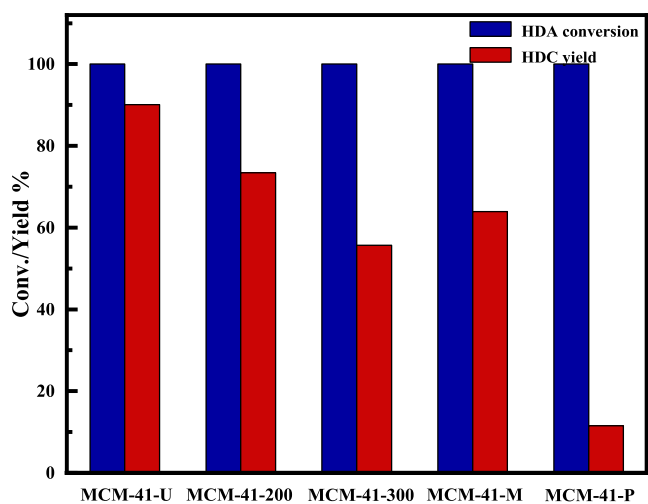


Figure 6.  $^1\text{H}$  MAS NMR spectra of five MCM-41 samples.

formed into isolated silanol groups by heat treatment.<sup>39</sup> The peaks at  $^1\text{H}$  chemical shifts of 1.01 and 2.66 ppm were observed for MCM-41-M. The peak at 1.01 ppm may be assigned to the isolated silanol group noninteracting with neighbors or bound water molecules at a silica surface.<sup>45</sup> For MCM-41-P, the strong peak signal was observed at 0 ppm, indicating that the amount of silanol group significantly decreases, probably due to the formation of Si-O-Si(Ph)<sub>3</sub>. This evidence indicated that the hydrogen-bonded and isolated silicone silanol group of MCM-41-U was shielded after being modified by TMCS and TPCS.

**3.3.2. Catalytic Performance of MCM-41 Samples.** The catalyst activities of MCM-41-U and modified MCM-41 samples were evaluated, and the results are summarized in Figure 7. It is found that when MCM-41-200 was used, the yield of HDC was 73.4%, and the yield of HDC obtained by using MCM-41-300 as a catalyst decreased to 55.7%. These findings suggested that high-temperature calcination would



**Figure 7.** Effect of five MCM-41 samples on carbonylation of HDA. Conditions:  $n_{\text{methanol}}/n_{\text{MC}}/n_{\text{HDA}} = 60:6:1$ , catalyst dosage = 10 wt % (based on HDA), temperature = 190 °C, time = 3 h.

reduce the catalytic performance of MCM-41. The decrease in the catalytic activity of MCM-41 after calcination may be attributed to the reduction in the number of silanol groups on MCM-41-200 and MCM-41-300, which was indicated by the results of characterization. Similar evidence was observed for the chlorosilane-modified MCM-41 samples. When MCM-41-M and MCM-41-P were used as the catalysts, the yields of HDC were 63.9 and 11.5%, respectively. According to the characterization results of MCM-41-P and MCM-41-M, the surface silanol groups of MCM-41-M and MCM-41-P may be hidden after modification with chlorosilane, resulting in a change in active species and sites on the catalysts. The poor catalytic performance of MCM-41-P may also be related to the destroyed pore structure of MCM-41-P and the reduced adsorption capacity, which was suggested by the results of  $N_2$  adsorption–desorption. As shown in Figure 3, the slopes of the isotherm of MCM-41-M and MCM-41-P decreased significantly in the multilayer adsorption stage ( $P/P_0$  in the range of 0.3–0.4), suggesting that the chlorosilane modification may affect the multilayer adsorption in the mesopores.<sup>46</sup> The performance of the catalyst indicated that the modification of MCM-41 by calcination and chlorosilane caused a decrease in the catalytic activity of MCM-41, implying that the abundant surface silanol groups on MCM-41 may be the vital promoting factor for HDC formation by carbonylation of HDA using MC as the carbonyl source.

To further understand the catalytic performance of MCM-41-U on carbonylation of HDA, *in situ* FTIR characterization was performed to observe the trends of the characteristic peaks of HDA, PU, and HDC under the conditions with the presence

of the catalyst. As described in Section 3.1, the formation of HDC from HDA and MC occurs *via* two steps with PU as the intermediate. First, HDA attacks the carbonyl carbon in MC to produce the intermediate PU, which happens quickly and easily. It is generally accepted that weak nucleophilic groups can be replaced by stronger ones. Therefore, the  $-OCH_3$  of MC may be easily replaced by the  $-NH_2$  of HDA, which is a stronger nucleophilic group than  $-OCH_3$ , in the process of the interaction of HDA and MC, resulting in the formation of PU. *In situ* FTIR characterization suggests that the presence of MCM-41-U could promote the alcoholysis of PU to HDC with methanol involving (Figure S4). This may be attributed to the presence of the silanol group on the surface of MCM-41-U. The silanol group may contribute to HDC synthesis in two ways: on the one hand, the silanol group may be able to interact with methanol to convert methanol into the methoxyl group;<sup>47</sup> then, the oxygen in the methoxyl group may attack the carbonyl carbon in PU. On the other hand, the silanol groups may promote the activation of the  $-NH_2$  group of MC or the  $-NH-$  group of PU,<sup>26</sup> thus accelerating the formation of HDC. Based on the characterizations and our previous work,<sup>48</sup> a possible reaction pathway and mechanism were proposed, as shown in Figure 8.

**3.4. Effect of Reaction Conditions on HDC Yield.** The effects of the reaction conditions, including the reaction temperature, molar ratio of raw materials (molar ratio of HDA and MC, as well as methanol dosage), catalyst dosage, and reaction time, were investigated. When the influence of one parameter was evaluated, the other parameters remained constant. The results are summarized in Figure 9. Since HDA can be converted even under noncatalytic conditions, only the effects of reaction conditions on the HDC yield are described here.

The effect of reaction temperature on the yield of HDC was investigated in the range of 180–195 °C, as shown in Figure 9a. The temperature has a significant impact on the yield of HDC. When the temperature increased from 180 to 190 °C, the yield of HDC increased from 37.2 to 90.1%. The increase in the HDC yield may be attributed to the accelerated reaction rate caused by a higher temperature. In addition, the formation of HDC belongs to the endothermic reaction, and thereby the formation of HDC will be promoted when the temperature is increased. However, when the reaction temperature further increased to 200 °C, the yield of HDC decreased from 90.1 to 26.8%. It probably results from the fact that a high temperature also leads to severe side reactions. In summary, the optimal reaction temperature is 190 °C.

In view of the influence of the molar ratio of raw materials on the yield of HDC synthesis, the influences of the molar ratio of HDA and MC, as well as the methanol dosage (molar ratio of methanol and HDA), on the yield of HDC were investigated. As can be seen in Figure 9b, the yield of HDC

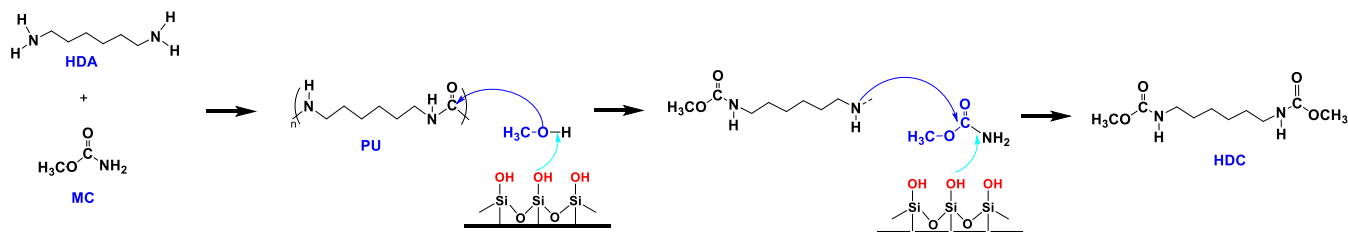


**Figure 8.** Possible reaction mechanism for the catalytic carbonylation of HDA with MC on MCM-41.

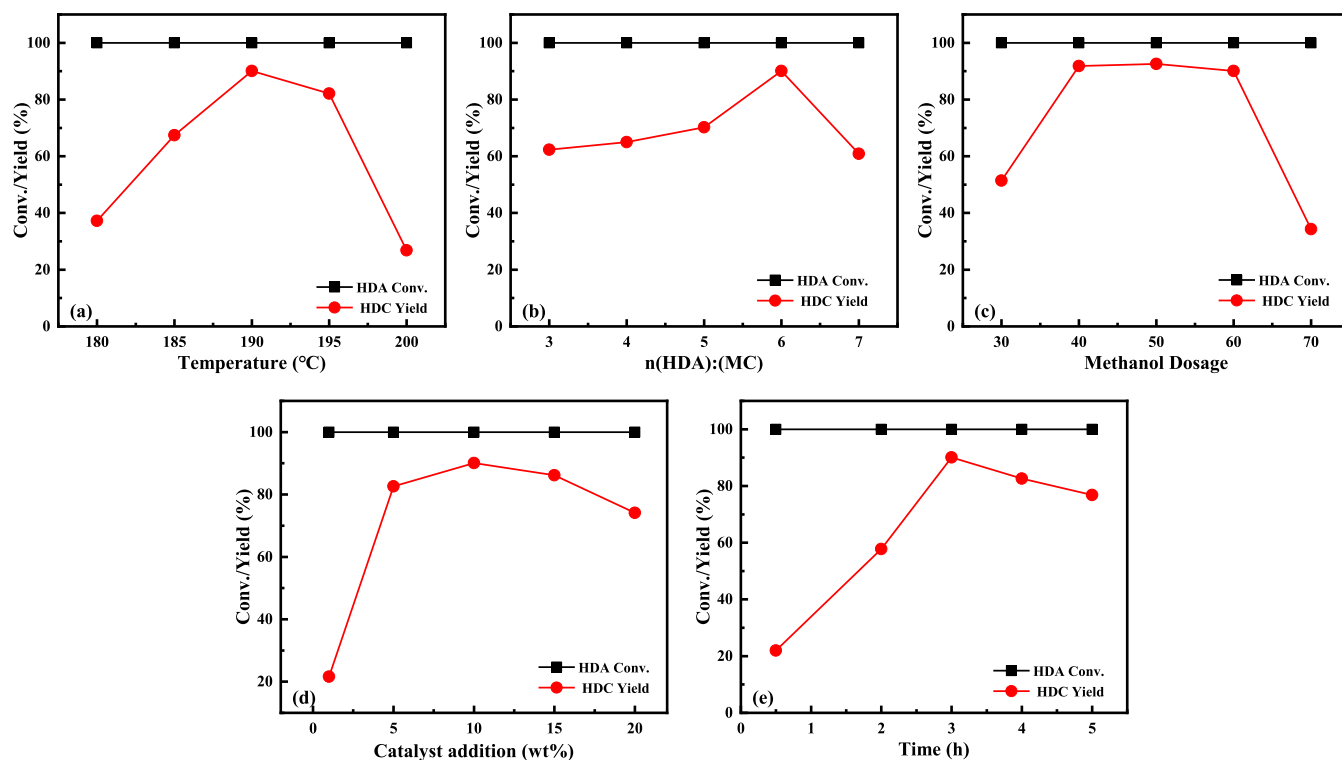


**Figure 9.** Effects of reaction condition on the yield of HDC. Conditions: (a)  $n_{\text{methanol}}/n_{\text{MC}}/n_{\text{HDA}} = 60:6:1$ , catalyst concentration = 10 wt % of HDA, time = 3 h; (b)  $n_{\text{methanol}}/n_{\text{HDA}} = 60:1$ , catalyst concentration = 10 wt % of HDA, temperature = 190 °C, time = 3 h; (c)  $n_{\text{MC}}/n_{\text{HDA}} = 6:1$ , catalyst concentration = 10 wt % of HDA, temperature = 190 °C, time = 3 h; (d)  $n_{\text{methanol}}/n_{\text{MC}}/n_{\text{HDA}} = 60:6:1$ , temperature = 190 °C, time = 3 h; and (e)  $n_{\text{methanol}}/n_{\text{MC}}/n_{\text{HDA}} = 60:6:1$ , catalyst concentration = 10 wt % of HDA, temperature = 190 °C.

increased from 62.3 to 90.1% when the molar ratio of HDA to MC increased from 1:3 to 1:6. High concentrations of MC will accelerate the reaction, thus promoting the reaction to proceed in the positive direction. However, when the molar ratio of HDA to MC was 1:7, the yield of HDC dropped to 60.9%. The possible reason was that the increase in the MC amount also promoted the methylation of HDA, resulting in an increase in byproducts, thereby leading to a decrease of the HDC yield. As shown in Figure 9c, the HDC yield increased from 51.4 to 91.8% as the methanol dosage increased from 30 to 40. The increase in the methanol dosage reduced the substrate concentration, thus inhibiting the side reaction. When the methanol dosage ratio was further increased from 40 to 60, the HDC yields were maintained at around 90%, and the highest HDA yield, which was 92.6%, was obtained at a methanol dosage of 50. When the methanol dosage ratio was adjusted to 70, the yield of HDC decreased rapidly. Utilization of a large amount of methanol will lower the concentration of the catalyst, reducing the contact chance between the catalyst and intermediate and thereby resulting in a low conversion rate of intermediate to HDC. In conclusion, the optimal molar ratio of HDA and MC and methanol dosage are 1:6:50, respectively.

The influence of the catalyst dosage on the yield of HDC was investigated, as presented in Figure 9d. The yield of HDC rapidly increased from 21.6 to 82.6% when the catalyst dosage increased from 1 to 5 wt % (based on HDA) and then slowly increased to a maximum of 90.1% when the catalyst dosage further increased to 10 wt %. It may be attributed to the fact that an increase in the catalyst dosage resulted in an increase in catalytic sites, promoting the formation of HDC. However, only 86.2% of HDC yield was obtained when the catalyst dosage was 15 wt % (based on HDA). Excessive catalyst may

cause partial dissociation of the carbamate bond of HDC, resulting in a decrease in the HDC yield. Therefore, the optimal catalyst dosage is 10 wt % (based on HDA).

Finally, the effect of the reaction time on the yield of HDC was investigated, and the results are shown in Figure 9e. The yield of HDC was 82.9% after 2 h, indicating that the catalyst has a high catalytic efficiency. With the extension of reaction time to 3 h, the HDC yield was as high as 93.3%. It may be explained by the reason that the intermediate polyurea was continuously converted into HDC as the reaction time was prolonged. However, the yield of HDC began to decline with the further extension of reaction time, which may be related to the thermal decomposition of HDC. In conclusion, the optimal reaction time is 3 h.

**3.5. Catalyst Stability.** The stability of the catalyst was evaluated through recycling five times, and the results are shown in Figure 10.

After every use, the catalyst was separated by centrifugation and directly used in the next run. Under the conditions with a reaction temperature of 190 °C, a molar ratio of HDA, MC, and methanol of 1:6:50, a catalyst dosage of 10 wt %, and a reaction time of 3 h, the yield of HDC decreased from 92.6 to 67.7% after four cycles and then the HDC yield was maintained at 67.9% in the fifth cycle. When the reaction time of the fifth cycle was extended from 3 to 5 h, the yield of HDC increased to 77.7%. The decrease in the activity of the catalyst after recycling may be due to the reduction of catalytic sites, resulting in the reduction of catalytic efficiency. The results of the catalyst leaching experiments (Figure S6) suggest that the catalyst leaching showed negligible effect on the HDC yield, implying that the leaching effect of MCM-41 was minor.

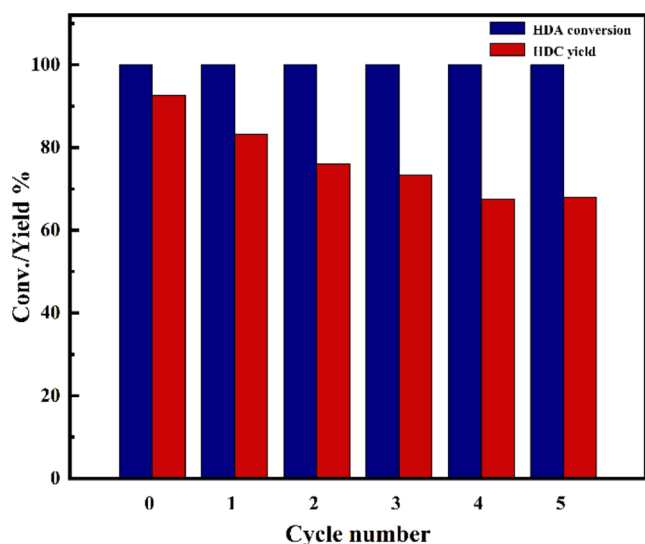


**Figure 10.** Reusability of MCM-41-U in carbonylation of HDA. Conditions:  $n_{\text{methanol}}/n_{\text{MC}}/n_{\text{HDA}} = 50:6:1$ , catalyst content = 10 wt % of HDA, temperature = 190 °C, time = 3 h.

In order to explore the reason for catalyst deactivation, the catalyst that recycled after five cycles, which was named MCM-41-R, was subjected to characterization. The results of  $\text{N}_2$  physical absorption/desorption of the fresh MCM-41 and MCM-41-R (Figure S7 and Table S1) showed that although the pore size of MCM-41-R was similar to the fresh catalyst,

the surface area and pore volume of MCM-41-R were significantly lower than that of MCM-41. These findings suggested that the catalyst has been agglomerated and that the pore structure of the particles may have been destroyed after use. Consistent with characterization results of  $\text{N}_2$  physical absorption/desorption, the agglomeration of MCM-41-R particles was observed by SEM images (Figure S8). The agglomeration may result from the interaction between the catalyst and reactant at high temperatures over a long period. The XRD pattern (Figure S9) showed that the intensities of (110) and (200) crystal plane diffraction peaks of MCM-41-R were significantly reduced, indicating that the highly ordered structure of MCM-41 deteriorated. The FTIR spectra (Figure S10) showed that the number of silanol groups on the catalyst surface was reduced after use, which was proved by the reduced intensities of the peaks at 3450  $\text{cm}^{-1}$  (hydrogen-bonded silanol group) and 1630  $\text{cm}^{-1}$  (O–H bending vibration). In the meantime, the absorption peaks at 2976  $\text{cm}^{-1}$  (stretching vibration of the C–H bond) and 2366  $\text{cm}^{-1}$  (stretching vibration of the Si–H bond) appeared. Similar findings can also be observed in the results of  $^1\text{H}$  MAS NMR, as shown in Figure S11. The spectra showed that the main peak chemical shift of MCM-41 moved to 2.28 ppm, indicating a reduced number of hydrogen-bonded silanol groups on the catalyst surface. The observation above implied that MC may interact with MCM-41 under high-temperature and high-pressure conditions, thus shielding a portion of the surface silanol groups on MCM-41 and leading to a decreased catalyst activity. The thermogravimetric (TG) curve of MCM-41

**Table 2.** Effect of MCM-41 on the N-Substituted Dicarbamate Synthesis

Entry <sup>a</sup>	Substrate	Product	Conversion (%)	Yield (%)
1			100	91.7
2			100	87.2*
3			100	90.9*
4			100	58.0
5			100	41.3
6			100	44.3*
7			100	88.1*
8			100	80.7*

<sup>a</sup>Reaction conditions: molar ratio of  $n_{\text{methanol}}/n_{\text{MC}}/n_{\text{HDA}} = 50:6:1$ , catalyst content = 10 wt % (based on diamine), reaction temperature = 190 °C, reaction time = 3 h. \* is the separation yield based on diamine.

(Figure S12) showed that MCM-41 was stable at temperatures below 900 °C. However, MCM-41-R experienced three stages of weight loss during heating to 900 °C. The three weight losses from low temperature to high temperature may be attributed to the removal of adsorbed methanol, the volatilization of the adsorbed product HDC, and the combustion of carbon deposits, respectively. In conclusion, the deactivation of the catalyst may be attributed to two factors. First, the change in the pore structure of the catalyst and the formation of a small amount of carbon deposits affected the adsorption and activation of the reactant molecules. Second, the reduction in the number of silanol groups in the catalyst led to a decrease in the catalytic activity.

**3.6. Substrate Scope.** Methylene diphenyl diisocyanate (MDI), toluene diamine (TDI), and phenylene diisocyanate (PPDI) are important aromatic isocyanates and are usually applied in the production of PU coatings. Typical aliphatic isocyanates, such as pentamethylene diisocyanate (PDI), isophorone diisocyanate (IPDI), hydrogenated phenyl dimethylene diisocyanate (H<sub>6</sub>XDI), hydrogenated diphenylmethane diisocyanate (H<sub>12</sub>MDI), and xylylene diisocyanate (XDI), are widely used in automobiles, coatings, medical instruments, and other industries. Therefore, the corresponding carbamates were synthesized over MCM-41 to investigate the limitation and scope of the catalyst. The results of the corresponding dicarbamate synthesis catalyzed by MCM-41 are summarized in Table 2.

As shown in Table 2, the conversions of all amines were 100%, while the yields of aliphatic and alicyclic carbamates generally were much higher than those of aromatic carbamates. For example, the yields of pentamethylene dicarbamate (PDC, entry 1), hydrogenated phenyl dimethylene dicarbamates (H<sub>6</sub>XDC, entry 2), hydrogenated diphenylmethane dicarbamates (H<sub>12</sub>MDC, entry 3), m-xylylene dicarbamate (XDC, entry 4), and isophorone dicarbamate (IPDC, entry 8) were 91.7, 87.2, 90.9, 58.0, and 80.7%, respectively. However, the yields of 4,4'-methylene diphenyl dicarbamate (MDC, entry 5) and 1,4-phenylene dicarbamate (PPDC, entry 6) were 41.3 and 44.3%, which were lower than the aliphatic/alicyclic carbamates. It is speculated that the interaction between the amino group, the electron-donating group, and the benzene ring in the aromatic amines through *p*- $\pi$  conjugation reduces the electron cloud density of the amino group, thereby lowering the reaction activity of the amino group. An exception was observed when toluene diamine (TDA, entry 7), an aromatic amine, was used as the substrate, and the yield of the corresponding dicarbamate reached 88.1%. The possible reason is that the connection of another electron-donating group -CH<sub>3</sub> to the benzene ring may increase the reactivity of the amino group in TDA. These findings demonstrated that MCM-41 exhibited good performance in synthesizing N-substituted dicarbamates, especially aliphatic/alicyclic carbamates.

## 4. CONCLUSIONS

In this work, MCM-41 was found to be an effective catalyst for the synthesis of HDC via the carbonylation reaction of HDA, MC, and methanol. The good performance of MCM-41 probably results from the abundance of silanol groups on the surface of MCM-41. The calcined MCM-41 and chlorosilane-modified MCM-41 were prepared to explore the effect of silanol groups on the catalytic activity. Characterizations based on FTIR and <sup>1</sup>H MAS NMR suggested that the number of

silanol groups on MCM-41 was reduced after calcination and chlorosilane modification, resulting in a decrease in catalytic activity. After five cycles of the MCM-41 catalyst, the HDC yield decreases from 92.6 to 67.9%. The characterization of the used catalyst revealed that the catalyst particles undergo agglomeration and carbon deposition, affecting the adsorption and activation of the reactant molecules on the catalyst. In addition, the reduction in the number of surface silanol groups on the catalyst also leads to a decrease in the catalytic activity.

## ■ ASSOCIATED CONTENT

### Supporting Information

The Supporting Information is available free of charge at <https://pubs.acs.org/doi/10.1021/acsomega.4c03437>.

Data treatment, reaction pathway analysis, pore size distribution of MCM-41 catalysts, leaching effect of the catalyst, and characterization of fresh and recycled catalysts (PDF)

## ■ AUTHOR INFORMATION

### Corresponding Author

**Liguo Wang** – CAS Key Laboratory of Green Process and Engineering, National Engineering Research Center of Green Recycling for Strategic Metal Resources, Institute of Process Engineering, Chinese Academy of Sciences, Beijing 100190, China; Sino-Danish College, University of Chinese Academy of Sciences, Beijing 100049, China; [orcid.org/0000-0002-8509-7950](https://orcid.org/0000-0002-8509-7950); Email: [lgwang@ipe.ac.cn](mailto:lgwang@ipe.ac.cn)

### Authors

**Junya Cao** – School of Chemical & Environmental Engineering, China University of Mining & Technology (Beijing), Beijing 100083, China

**Liyan Zhao** – CAS Key Laboratory of Green Process and Engineering, National Engineering Research Center of Green Recycling for Strategic Metal Resources, Institute of Process Engineering, Chinese Academy of Sciences, Beijing 100190, China

**Xiaoxuan Wang** – School of Chemical & Environmental Engineering, China University of Mining & Technology (Beijing), Beijing 100083, China; CAS Key Laboratory of Green Process and Engineering, National Engineering Research Center of Green Recycling for Strategic Metal Resources, Institute of Process Engineering, Chinese Academy of Sciences, Beijing 100190, China

**Shuang Xu** – CAS Key Laboratory of Green Process and Engineering, National Engineering Research Center of Green Recycling for Strategic Metal Resources, Institute of Process Engineering, Chinese Academy of Sciences, Beijing 100190, China

**Yan Cao** – CAS Key Laboratory of Green Process and Engineering, National Engineering Research Center of Green Recycling for Strategic Metal Resources, Institute of Process Engineering, Chinese Academy of Sciences, Beijing 100190, China

**Peng He** – CAS Key Laboratory of Green Process and Engineering, National Engineering Research Center of Green Recycling for Strategic Metal Resources, Institute of Process Engineering, Chinese Academy of Sciences, Beijing 100190, China; [orcid.org/0000-0002-1479-8717](https://orcid.org/0000-0002-1479-8717)

Complete contact information is available at: <https://pubs.acs.org/10.1021/acsomega.4c03437>

## Author Contributions

J.C.: conceptualization, methodology. L.Z.: writing—review and editing, conceptualization. X.W.: writing—original draft, investigation, data curation. S.X.: investigation, data curation. Y.C.: supervision. P.H.: funding acquisition. L.W.: supervision, funding acquisition.

## Author Contributions

<sup>||</sup>J.C., L.Z., and X.W. contributed equally to this work and should be considered cofirst authors.

## Notes

The authors declare no competing financial interest.

## ACKNOWLEDGMENTS

This work was financially supported by the Clean Combustion and Low-carbon Utilization of Coal, Strategic Priority Research Program of the Chinese Academy of Sciences, Grant No. XDA 29000000.

## REFERENCES

- (1) Ghosh, A. K.; Brindisi, M. Organic carbamates in drug design and medicinal chemistry. *J. Med. Chem.* **2015**, *58* (7), 2895–2940.
- (2) Hyun, M. J.; Shin, M.; Kim, Y. J.; Suh, Y.-W. Phosgene-free decomposition of dimethylhexane-1,6-dicarbamate over ZnO. *Res. Chem. Intermed.* **2016**, *42* (1), 57–70.
- (3) Duan, C. W.; You, J.; Liu, B.; Ma, J. L.; Zhou, H. P.; Zhang, H. B.; Zhang, J. Ionic liquid-mediated solvothermal synthesis of 4,4'-methylenebis(diphenyl diisocyanate (MDI): an efficient and environment-friendly process. *New J. Chem.* **2018**, *42* (14), 12243–12255.
- (4) Zhao, L.; He, P.; Wang, L.; Ammar, M.; Cao, Y.; Li, H. Catalysts screening, optimization and mechanism studies of dimethylhexane-1,6-dicarbamate synthesis from 1,6-hexanediamine and dimethyl carbonate over Mn(OAc)<sub>2</sub> catalyst. *Catal. Today* **2017**, *281*, 392–401.
- (5) Wang, P.; Fei, Y.; Li, Q.; Deng, Y. Effective synthesis of dimethylhexane-1,6-dicarbamate from 1,6-hexanediamine and dimethyl carbonate using 3-amino-1,2,4-triazole potassium as a solid base catalyst at ambient temperature. *Green Chem.* **2016**, *18* (24), 6681–6686.
- (6) Alferov, K. A.; Fu, Z.; Ye, S.; Han, D.; Wang, S.; Xiao, M.; Meng, Y. One-Pot Synthesis of Dimethyl Hexane-1,6-diyldicarbamate from CO<sub>2</sub>, Methanol, and Diamine over CeO<sub>2</sub> Catalysts: A Route to an Isocyanate-Free Feedstock for Polyurethanes. *ACS Sustainable Chem. Eng.* **2019**, *7* (12), 10708–10715.
- (7) Heath, R. Isocyanate-Based Polymers. In *Brydson's Plastics Materials*, 8th ed.; Butterworth-Heinemann: Oxford, 2017; pp 799–835.
- (8) Wang, G.; Li, K.; Zou, W.; Hu, A.; Hu, C.; Zhu, Y.; Chen, C.; Guo, G.; Yang, A.; Drumright, R.; Argyropoulos, J. Synthesis of HDI/IPDI hybrid isocyanurate and its application in polyurethane coating. *Prog. Org. Coat.* **2015**, *78*, 225–233.
- (9) Cao, Y.; He, L.; Xia, C. Oxidative Carbonylation of Amines. In *The Chemical Transformations of C1 Compounds*; Wiley-VCH GmbH: Weinheim, 2022; pp 687–720.
- (10) Leung, T. W.; Dombek, B. D. Oxidative Carbonylation of Amines Catalyzed by Metallomacrocyclic Compounds. *J. Chem. Soc., Chem. Commun.* **1992**, *3*, 205–206.
- (11) Tafesh, A. M.; Weiguny, J. A review of the selective catalytic reduction of aromatic nitro compounds into aromatic amines, isocyanates, carbamates, and ureas using CO. *Chem. Rev.* **1996**, *96* (6), 2035–2052.
- (12) Shi, F.; He, Y.; Li, D.; Ma, Y.; Zhang, Q.; Deng, Y. Developing effective catalyst system for reductive carbonylation of nitrobenzene based on the diversity of ionic liquids. *J. Mol. Catal. A: Chem.* **2006**, *244* (1–2), 64–67.
- (13) Yu, T.; Si, Y.; Zhou, J.; Liu, M. Synthesis mechanism of dimethylhexane-1,6-dicarbamate from 1,6-hexamethylenediamine, urea and methanol: A molecular scale study based on density functional theory. *J. Mol. Graphics Modell.* **2023**, *118*, No. 108349.
- (14) Wang, P.; Liu, S.; Deng, Y. Important Green Chemistry and Catalysis: Non-phosgene Syntheses of Isocyanates – Thermal Cracking Way. *Chin. J. Chem.* **2017**, *35* (6), 821–835.
- (15) Li, J.; Qi, X.; Wang, L.; He, Y.; Deng, Y. New attempt for CO<sub>2</sub> utilization: One-pot catalytic syntheses of methyl, ethyl and n-butyl carbamates. *Catal. Commun.* **2011**, *12* (13), 1224–1227.
- (16) Morais, D. C.; da Silva, M. J. Tin-Catalyzed Urea Alcoholysis With  $\beta$ -Citronellol: A Simple and Selective Synthesis of Carbamates. *Catal. Lett.* **2016**, *146* (8), 1517–1528.
- (17) Zhang, H.; Guo, X.; Zhang, Q.; Ma, Y.; Zhou, H.; Li, J.; Wang, L.; Deng, Y. Synthesis of dialkyl hexamethylenedicarbamate from 1,6-hexamethylenediamine and alkyl carbamate over Y(NO<sub>3</sub>)<sub>3</sub>·6H<sub>2</sub>O catalyst. *J. Mol. Catal. A: Chem.* **2008**, *296* (1–2), 36–41.
- (18) Guo, X.; Shang, J.; Ma, X.; Li, J.; Zhang, H.; Cui, X.; Shi, F.; Deng, Y. Synthesis of dialkyl hexamethylene-1,6-dicarbamate from 1,6-hexamethylenediamine and alkyl carbamate over FeCl<sub>3</sub> as catalyst. *Catal. Commun.* **2009**, *10* (8), 1248–1251.
- (19) Han, B.; Zhao, W.; Qin, X.; Li, Y.; Sun, Y.; Wei, W. Synthesis of dimethyl hexane-1,6-diyldicarbamate from 1,6-hexamethylenediamine and methyl carbamate using lead dioxide as catalyst. *Catal. Commun.* **2013**, *33*, 38–41.
- (20) Cao, Y.; Li, H.; Li, X.; Wang, L.; Zhu, G.; Tang, Q. Heterogeneous synthesis of dimethylhexane-1,6-dicarbamate from 1,6-hexanediamine and methyl carbonate in methanol over a CeO<sub>2</sub> catalyst. *Chin. J. Chem. Eng.* **2015**, *23* (2), 446–450.
- (21) Shang, J.; Guo, X.; Shi, F.; Ma, Y.; Zhou, F.; Deng, Y. N-substituted carbamates syntheses with alkyl carbamate as carbonyl source over Ni-promoted Fe<sub>3</sub>O<sub>4</sub> catalyst. *J. Catal.* **2011**, *279* (2), 328–336.
- (22) Hui, X.; Wang, L.; Cao, Y.; Xu, S.; He, P.; Li, H. Highly efficient synthesis of novel bio-based pentamethylene dicarbamate via carbonylation of pentanediamine with ethyl carbamate over well-defined titanium oxide catalysts. *Catal. Sci. Technol.* **2022**, *12* (7), 2315–2327.
- (23) Cao, J.; Zhou, J.; Wang, L.; Cao, Y. Effective Synthesis of m-Xylylene Dicarbamate via Carbonylation of m-Xylylene Diamine with Ethyl Carbamate over Hierarchical TS-1 Catalysts. *ACS Omega* **2022**, *7* (27), 23851–23857.
- (24) Martínez-Edo, G.; Balmori, A.; Pontón, I.; Martí del Río, A.; Sánchez-García, D. Functionalized Ordered Mesoporous Silicas (MCM-41): Synthesis and Applications in Catalysis. *Catalysts* **2018**, *8* (12), 617–679.
- (25) Valiey, E.; Dekamin, M. G.; Alirezvani, Z. Sulfamic acid pyromellitic diamide-functionalized MCM-41 as a multifunctional hybrid catalyst for melting-assisted solvent-free synthesis of bioactive 3,4-dihydropyrimidin-2-(1H)-ones. *Sci. Rep.* **2021**, *11* (1), No. 11199.
- (26) Toor, S. K.; Kushwaha, J. P.; Sangal, V. K. Aromatic amines equilibrium sorptive interaction with synthesized silica based mesoporous MCM-41: Physicochemical evaluation and isotherm modeling. *J. Environ. Sci. Health, Part A: Toxic/Hazard. Subst. Environ. Eng.* **2019**, *54* (4), 286–294.
- (27) Gao, Y.; Chen, H.; Tay-Agbozo, S.; Kispert, L. D. Photo-induced electron transfer of carotenoids in mesoporous sieves (MCM-41) and surface modified MCM-41: The role of hydrogen bonds on the electron transfer. *J. Photochem. Photobiol., A* **2017**, *341*, 1–11.
- (28) Chen, J.; Li, Q.; Xu, R.; Xiao, F. Distinguishing the Silanol Groups in the Mesoporous Molecular Sieve MCM-41. *Angew. Chem. Int. Ed.* **1996**, *34* (23–24), 2694–2696.
- (29) Shang, J.; Liu, S.; Ma, X.; Lu, L.; Deng, Y. A new route of CO<sub>2</sub> catalytic activation: syntheses of N-substituted carbamates from dialkyl carbonates and polyureas. *Green Chem.* **2012**, *14* (10), 2899–2906.
- (30) Karl, M.; Kalyakina, A.; Dräger, C.; Haufe, S.; Pokrant, S. Porous MCM-41 Silica Materials as Scaffolds for Silicon-based Lithium-ion Battery Anodes. *ChemElectroChem* **2024**, *11* (7), No. e202300707.
- (31) Sun, L. N.; Lu, L. X.; Qiu, X. L.; Tang, Y. L. Development of low-density polyethylene antioxidant active films containing  $\alpha$ -

tocopherol loaded with MCM-41 (Mobil Composition of Matter No. 41) mesoporous silica. *Food Control* **2017**, *71*, 193–199.

(32) Wouters, B. H.; Chen, T.; Dewilde, M.; Grobet, P. J. Reactivity of the surface hydroxyl groups of MCM-41 towards silylation with trimethylchlorosilane. *Microporous Mesoporous Mater.* **2001**, *44–45*, 453–457.

(33) Jafarzadeh, A.; Sohrabnezhad, S.; Zanjanchi, M. A.; Arvand, M. Fabrication of MCM-41 fibers with well-ordered hexagonal mesostructure controlled in acidic and alkaline media. *J. Solid State Chem.* **2016**, *242*, 236–242.

(34) Branton, P. J.; Hall, P. G.; Sing, K. S.; Reichert, H.; Schüth, F.; Unger, K. K. Physisorption of argon, nitrogen and oxygen by MCM-41, a model mesoporous adsorbent. *J. Chem. Soc., Faraday Trans.* **1994**, *90* (19), 2965–2967.

(35) Li, C. C.; Qiao, X. C.; Yu, J. G. Large surface area MCM-41 prepared from acid leaching residue of coal gasification slag. *Mater. Lett.* **2016**, *167*, 246–249.

(36) Li, X. D.; Zhai, Q. Z. Characterization of methylated nanoscale MCM-41 material. *J. Iran. Chem. Soc.* **2011**, *8* (1), S1–S8.

(37) Sohrabnezhad, S.; Jafarzadeh, A.; Pourahmad, A. Synthesis and characterization of MCM-41 ropes. *Mater. Lett.* **2018**, *212*, 16–19.

(38) Jentys, A.; Kleestorfer, K.; Vinek, H. Concentration of surface hydroxyl groups on MCM-41. *Microporous Mesoporous Mater.* **1999**, *27* (2–3), 321–328.

(39) Zhao, X. S.; Lu, G. Q.; Whittaker, A. K.; Millar, G. J.; Zhu, H. Y. Comprehensive Study of Surface Chemistry of MCM-41 Using <sup>29</sup>Si CP/MAS NMR, FTIR, Pyridine-TPD, and TGA. *J. Phys. Chem. B* **1997**, *101* (33), 6313–6660.

(40) Wang, Z.; Jiang, Y.; Zhang, Y.; Shi, J.; Stampfl, C.; Hunger, M.; Huang, J. Identification of Vicinal Silanols and Promotion of Their Formation on MCM-41 via Ultrasonic Assisted One-Step Room-Temperature Synthesis for Beckmann Rearrangement. *Ind. Eng. Chem. Res.* **2018**, *57* (16), 5550–5557.

(41) Wang, Z.; Ling, H.; Shi, J.; Stampfl, C.; Yu, A.; Hunger, M.; Huang, J. Acidity enhanced [Al]MCM-41 via ultrasonic irradiation for the Beckmann rearrangement of cyclohexanone oxime to  $\epsilon$ -caprolactam. *J. Catal.* **2018**, *358*, 71–79.

(42) Wouters, B. H.; Chen, T. H.; Dewilde, M.; Grobet, P. J. Reactivity of the surface hydroxyl groups of MCM-41 towards silylation with trimethylchlorosilane. *Microporous Mesoporous Mater.* **2001**, *44–45*, 453–457.

(43) Kovalchuk, T. V.; Sfihi, H.; Korchev, A. S.; Kovalenko, A. S.; Il'in, V. G.; Zaitsev, V. N.; Fraissard, J. Synthesis, structure, and acidic properties of MCM-41 functionalized with phosphate and titanium phosphate groups. *J. Phys. Chem. B* **2005**, *109* (29), 13948–13956.

(44) Trébosc, J.; Wiench, J. W.; Huh, S.; Lin, V. S.; Pruski, M. Solid-state NMR study of MCM-41-type mesoporous silica nanoparticles. *J. Am. Chem. Soc.* **2005**, *127* (9), 3057–3068.

(45) Protsak, I. S.; Morozov, Y. M.; Zhang, D.; Gun'ko, V. M. Surface Chemistry of Nanohybrids with Fumed Silica Functionalized by Polydimethylsiloxane/Dimethyl Carbonate Studied Using <sup>1</sup>H, <sup>13</sup>C, and <sup>29</sup>Si Solid-State NMR Spectroscopy. *Molecules* **2021**, *26* (19), No. 5974.

(46) Li, S.; Zhang, Y.; Xiang, K.; Chen, J.; Wang, J. Designing a novel type of multifunctional soil conditioner based on 4-arm star-shaped polymer modified mesoporous MCM-41. *Colloids Surf., A* **2022**, *648*, No. 129137.

(47) Ichihashi, H.; Ishida, M.; Shiga, A.; Kitamura, M.; Suzuki, T.; Suenobu, K.; Sugita, K. The catalysis of vapor-phase Beckmann rearrangement for the production of  $\epsilon$ -caprolactam. *Catal. Surv. Asia* **2003**, *7* (4), 261–270.

(48) Cao, J.; Wang, X.; Wang, L.; Cao, Y.; Hui, X.; He, P.; Li, H. Efficient synthesis of dimethyl hexane-1,6-dicarbamate via methoxycarbonylation of 1, 6-hexanediamine with methyl carbamate over acid-base enhanced CeO<sub>2</sub>. *Mol. Catal.* **2023**, *549*, No. 113453.